CHAPTER 2

KINETIC STUDIES OF HYDROGEN OXIDATION BY COBALOXIMES

Introduction

Cobaloximes as HER Catalysts

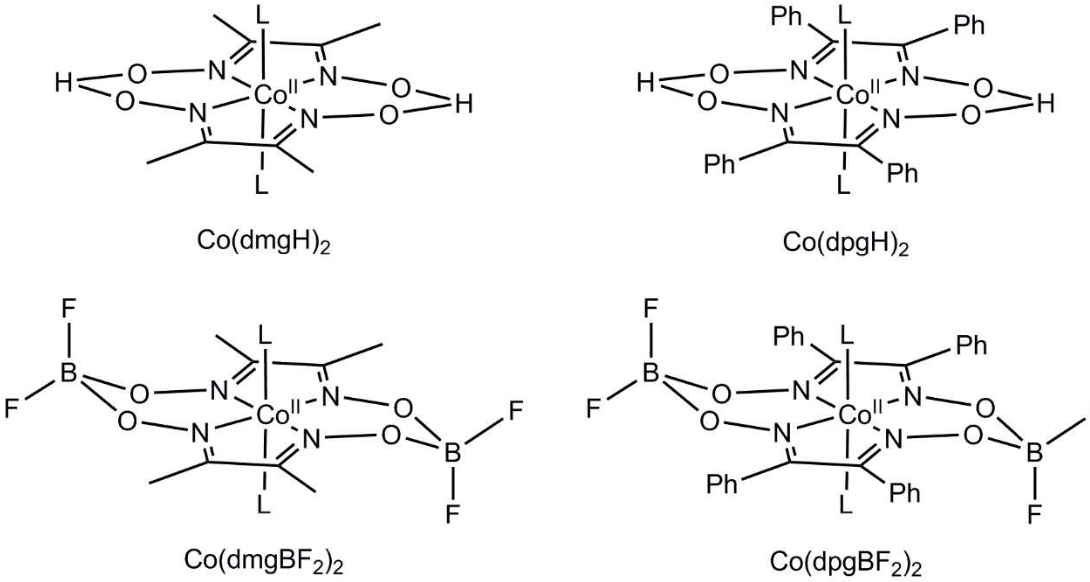

Chart 1: Cobaloxime complexes. L is typically solvent or pyridine.

In 1966, the first "cobaloximes" were synthesized by Schrauzer and Windgassen as models of the reduced form of vitamin B_{12}, and they coined the term for this family of molecules by analogy to "cobalamin".[1] The reaction of dimethylglyoxime (usually abbreviated $dmgH_2$) with cobaltous acetate resulted in the formation of a hydrogen-bonded macrocyclic complex, $Co(dmgH)_2L_2$, where the axial L sites are kinetically labile and usually occupied by solvent molecules. The remaining protons in the macrocycle can be replaced by BF_2 on reaction with

BF_3•Et_2O,[2] and the resulting complexes are generally much more stable, particularly in acid solution. Both reactions are quite general, and a number of similar complexes have been synthesized with varying substituents in the "backbone" of the diglyoxime macrocycle (Chart 1).[3]

Connolly and Espenson demonstrated in 1986 that trace amounts of $Co(dmgBF_2)_2L_2$ catalyzed the evolution of H_2 from acidic aqueous solutions of sufficiently reducing M(II) salts (M = Cr, Eu, V).[4] They reported that the reaction slowed considerably in the absence of halide ions, leading them to conclude that the rate limiting step was inner-sphere electron transfer in a halide-bridged intermediate. Without rate-limiting H-H bond formation, the authors were unable to interrogate the mechanism of that step, and so they proposed two possible routes proceeding from a Co(III) hydride intermediate formed by the protonation of the reduced Co(I) form of the catalyst (Scheme 1, red and blue arrows).

Scheme 1. Reproduced from reference 5 with permission from the copyright holder, American Chemical Society.

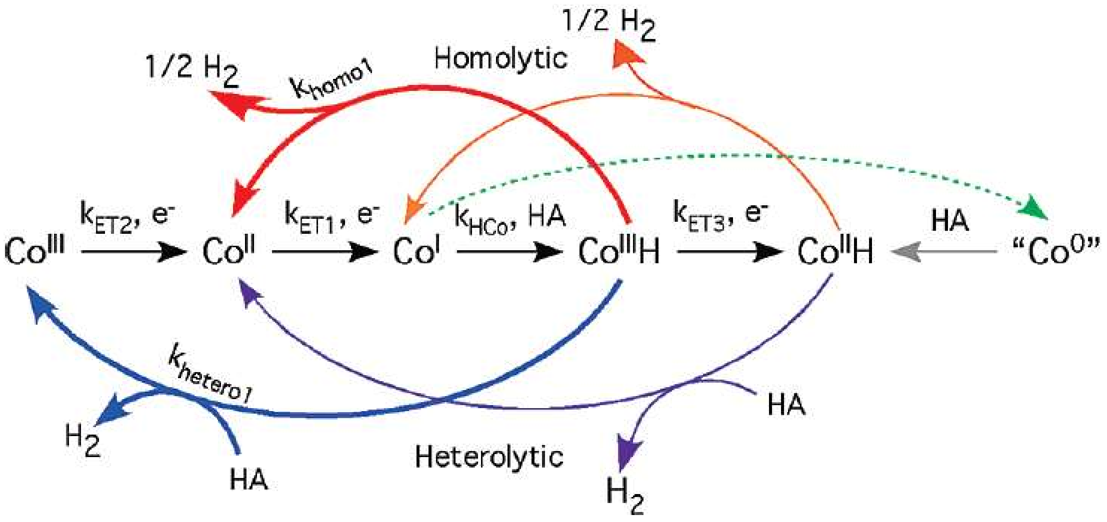

This result was not further investigated until 2005, when both the Artero[3] and Peters[6] groups reported nonaqueous electrocatalytic proton reduction using cobaloxime catalysts. Artero and coworkers found that $Co(dmgH)_2(py)Cl$ electrocatalyzes HER from triethylammonium chloride in DMF (pK_a = 10.75) at the Co(II/I) couple (-0.98 V vs. Ag/AgCl). Notably, they report that substitution of BF_2 for the bridging protons or H or Ph for the backbone methyls shifted the Co(II/I) couple anodically by ca. 100 mV, but shut down catalysis, suggesting that the Co(I) species formed were no longer basic enough to be protonated by triethylammonium. The authors considered the same general scheme as Connolly and Espenson, and concluded based on simulations of the cyclic voltammagrams that the heterolytic mechanism (Scheme 1, blue arrow) predominated under their catalytic conditions.

In contrast, the Peters group found that the fluoroborated derivative $Co(dmgBF_2)_2(MeCN)_2$ was a competent electrocatalyst for HER from trifluoroacetic acid (TFA) in MeCN (pK_a = 12.7) at the Co(II/I) couple (-0.55 V vs. SCE). They also reported that the diphenylglyoxime congener $Co(dpgBF_2)_2(MeCN)_2$ was a competent HER catalyst, but that the positive shift in the Co(II/I) couple relative to the methyl variant requires use of a stronger acid ($HBF_4 \bullet Et_2O$, pK_a = 0.1) to maintain activity; neither complex showed activity when a weaker acid such as benzoic acid (pK_a = 20.7) or TFA, respectively. Similar to Artero et al., Peters et al. used simulations of the catalytic cyclic voltammagrams to examine the mechanism of HER, but they concluded that the hemolytic mechanism (Scheme 1, red arrow) predominated for $Co(dmgBF_2)_2(MeCN)_2$ and were unable to distinguish between the two mechanisms for $Co(dpgBF_2)_2(MeCN)_2$.

This pair of reports sparked a general interest in the use of cobaloximes for HER in a variety of contexts, including photocatalytic[7–19] as well as electrocatalyic[3,5,6,20] systems in both aqueous and organic solvents. Despite the ubiquity of these reports, however, a consensus mechanism never developed.

There have been attempts to directly study the mechanism of cobaloxime-mediated HER, though the emerging picture has possibly become less clear rather than more. A 1971 report by Schrauzer and Holland[21] identifying a “hydridocobaloxime” prepared by reduction with $NaBH_4$ and stabilized by PBu_3 trans to the hydride (Chart 2) has formed the basis for mechanistic work from this apparent trapped intermediate. However, Artero et al. called into question the assignment of this complex as a classical metal hydride based on its purple color and the downfield ^{1}H NMR resonance (~6 ppm) assigned as that of the hydride; a Co(III) hydride would be expected to be pale yellow with a hydride resonance upfield of 0 ppm.[22] After repeating the experimental measurements and performing theoretical calculations, Artero reassigned the product as the ligand-protonated Co(I) tautomer of the original formulation with a hydride resonance of ~-5 ppm.

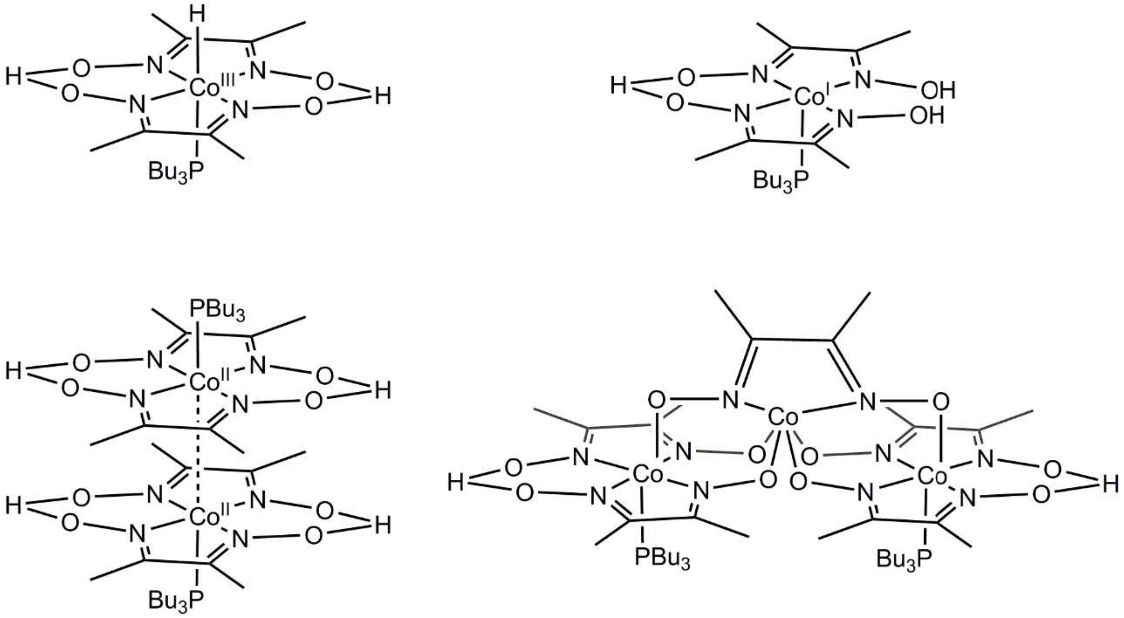

Chart 2: Assignments of the structure of "hydridocobaloxime". Top left, original assignment by Schrauzer and Holland;[21] top right, reassignment by Artero et al.;[22] bottom, major and minor products as assigned by Peters et al.[23]

More recently, the Peters group has again repeated that experimental characterization and found that the purple material which results from the $NaBH_4$ reduction of $Co(dmgH)_2Cl(PBu_3)$ does not correspond to a "hydridocobalxime" at all.[23] Instead, the major product was confirmed by X-ray crystallography to be the Co-Co bonded dimer $[Co(dmgH)_2(PBu_3)]_2$, with the apparent hydride signal arising from a paramagnetic trinuclear minor product. Alarmingly, this result invalidates mechanistic work which relied on this incorrectly assigned “hydride”, including studies which measured the rate of H_2 evolution from the material upon addition of acid[24] as well as studies which assigned the spectra of various intermediates based on the spectrum of “hydridocobaloxime”.[25]

The most direct inspection of the mechanism of cobaloxime-mediated HER is a contribution from Dempsey and Gray in 2010 utilizing a strong photoacid and transient absorption spectroscopy to rapidly protonate $[Co^I(dmgBF_2)_2(MeCN)]^-$, allowing for the observation of the formation and decay of two intermediates prior to H_2 evolution and generation of the Co(II).[26] These intermediates were proposed to correspond first to the Co(III) hydride which results from protonation of the Co(I) anion, followed by the intermediate Co(II) hydride which results from reduction by excess Co(I). This final species is ultimately protonated again to release H_2. This result demonstrated that further reduction of a Co(III) hydride is possible under catalytic conditions and may be necessary in order to render the metal hydride reactive enough to produce hydrogen. This pathway has more recently been proposed under electrocatalytic conditions based on foot-of-the-wave analysis and other electroanalytical chemistry methods.[27,28] With this possibility under consideration, a second homolytic path (Scheme 1, violet arrow) may be added to the possibilities first proposed by Schrauzer.

Also complicating the picture is the possibility for ligand noninnocence. The Peters group has investigated related macrocycles in which the oxime oxygens and bridging atoms on one half of the macrocycle have been replaced by hydrocarbon linkers (Chart 3), and these studies have highlighted the importance of ligand protonation in H-bridged cobaloxime systems.[29] Aqueous HER catalysis by these complexes shows a Nernstian response consistent with a one-proton, one-electron process, while catalysis by $Co(dmgBF_2)_2$ complexes in MeCN does not, suggesting that protonation likely occurs on the ligand.

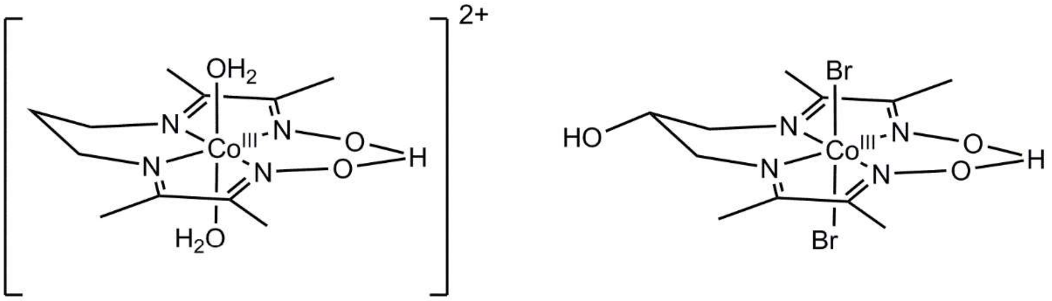

Chart 3: Cobalt diimine-dioxime complexes.

Additionally, a report by the Norton group concerning high-pressure spectroscopy of $Co(dmgBF_2)_2(MeCN)_2$ under 70 atm H_2 features slow growth of optical and ^1H NMR spectral features consistent with a solvent-assisted ligand-protonated product, suggesting that a ligand-protonated species could figure into catalysis even in the fluoroborated cobaloximes.[30] Electrochemical analysis of $Co(dmgBF_2)_2(MeCN)_2$ under high pressures of H_2, however, cast doubt on this hypothesis, as the $Co^{II/I}$ couple is positioned ca. 300 mV more negative than at 1 atm, which suggests that ligand-protonated species would not be the observed catalyst even if it is generated.[27]

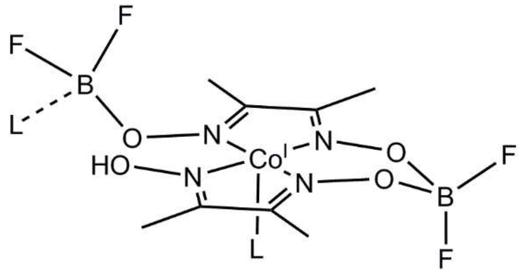

Figure 1: Proposed structure of the high-pressure reaction between H_2 and $Co(dmgBF_2)_2(MeCN)_2$ (L = MeCN).

History of Cobaloximes as Hydrogenation and HOR Catalysts

In the 1970s, the Simándi and Yamaguchi groups reported the first reactions of cobaloximes with dihydrogen, which resulted in decomposition via hydrogenation of the macrocyclic ligand.[31–34] This decomposition can be outcompeted by catalytic hydrogenation if an alternate substrate such as a Schiff base[35] or styrene[32] is present. Simándi et al. reported that the rate law for hydrogenation of styrene in MeOH and 1:1 MeOH:H_2O is second-order in $Co(dmgH)_2$ and first-order in H_2, suggesting that the turnover-limiting step is homolytic activation of H_2. They also reported that coordination of an axial pyridine in lieu of solvent (MeOH/H_2O) enhanced the reaction rate by two orders of magnitude, highlighting the importance of understanding the effect of the axial ligands in cobaloxime systems. Complicating the matter, under most conditions the resting state of the cobaloxime is Co(II), a labile oxidation state that lends the molecule to readily undergo axial ligand substitution, leading to speciation if more than one viable ligand exists in solution.[36] Similar axial ligand effects have surfaced in more recent years in both the HER[12,37,38] and H_2 activation[39] literature.

Simándi et al. also studied the reaction of $Co(dmgH)_2$ complexes with H_2 in the presence of strong Brønsted base and found it competent for HOR catalysis.[31] As with styrene, the observed rate law is termolecular, but the HOR rate is enhanced relative to styrene hydrogenation, which implies that they cannot have the same intermediate in the rate-limiting step. Simándi et al. propose that deprotonation of one of the macrocyclic bridges produces a more active species for H_2 activation, a suggestion which mirrors more recent observations of ligand protonation in HER.

Norton et al. have more recently developed $Co(dmgBF_2)_2$ complexes under H_2 as H-atom transfer catalysts for radical cyclizations.[40] Kinetics experiments with a modified trityl radical and with TEMPO as H-atom acceptors resulted in a rate law second-order in Co, first-order in H_2, and independent of acceptor concentration or identity. This result suggests that substitution of BF_2 at the bridging position does not change the turnover-limiting H_2 activation found by Simándi et al. Further detailed mechanistic work from the Norton group has established that only the pentacoordinate $Co(dmgBF_2)_2L$ is active, and that the identity of L can have a dramatic effect on the rate of reaction.[39] Stronger donor ligands which labilize the trans ligand can case as much as an order of magnitude rate enhancement. By contrast, the rate is slowed by an order of magnitude by PPh_3, which only singly ligates

$Co(dmgBF_2)_2$, which they attribute to enforcement of a pseudo-boat conformation in the macrocycle rather than the pseudo-chair observed in most crystal structures. The pseudo-boat conformation may be sterically congested enough to slow bimolecular activation of H_2.

Studies of HOR in organic solvent with fluoroborated cobaloximes have been limited to a stoichiometric demonstration by the Peters group that with $Co(dmgBF_2)_2(MeCN)_2$, but not $Co(dpgBF_2)_2(MeCN)_2$, some degree of reversibility is possible using the conjugate bases of the acids used for HER catalysis.[20] The reaction approaches an unfavorable ($K_{eq} = 0.03$ atm$^{-1/2}$) equilibrium over the course of 34 with anisosbestic behavior, which the authors attribute to decomposition of the complex.

Taken together, these reports display that the rate cobaloxime-mediated H_2 activation in both HOR and hydrogenation reactions are markedly sensitive to changes in both the macrocycle and axial ligands. The third-order rate constants found by Simándi et al. range from ~10-3200 $M^{-2}s^{-1}$ for styrene hydrogenation by $Co(dmgH)_2$, depending on the solvent and presence of added pyridine.[32] When the reaction is instead HOR with strong base, they found a third-order rate constant of ~2200 $M^{-2}s^{-1}$.[31] In MeCN, Norton et al. found a third-order rate constant of ~110 $M^{-2}s^{-1}$ for radical hydrogenation.[40] This relatively slow oxidation of H_2 in acetonitrile contrasts with the fast second-order rates (k_{app} = 7000 $M^{-1}s^{-1}$) observed for $Co(dmgBF_2)_2(MeCN)_2$-catalyzed HER.[6] Additional research is needed to clarify the mechanism of cobaloxime-mediated HER and HOR and the factors governing the reaction rates.

Results

Scheme 2

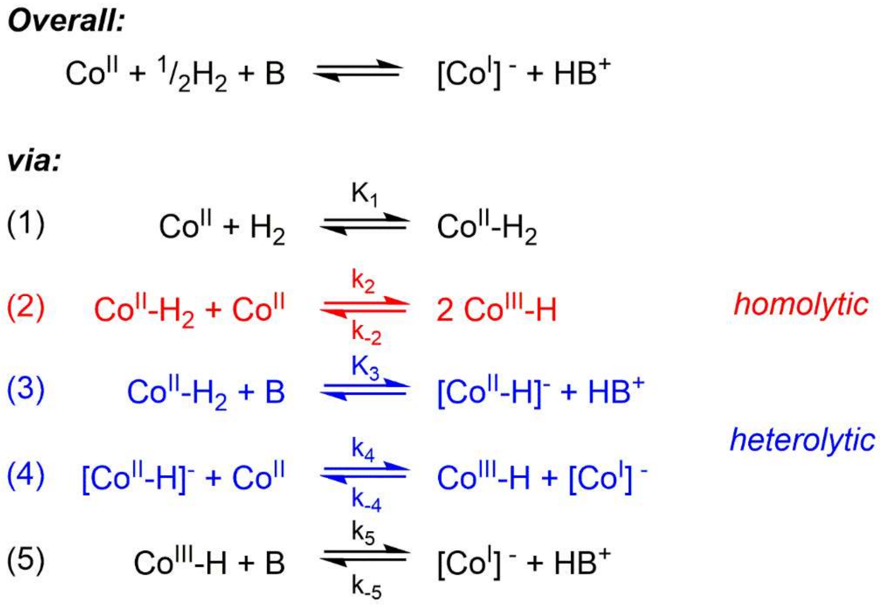

The stoichiometric oxidation of hydrogen to protons by cobaloximes may proceed either via bimetallic homolytic H-H bond cleavage or deprotonation (heterolysis), and the balance of data in the literature suggests that both pathways are accessible (Scheme 2). Using the pre-equilibrium approximation for equations (1) and (3) and the steady-state approximation for [Co^{III}-H], a rate law emerges which is second-order in Co regardless of the dominant pathway (Equation 6). In this work, kinetic studies of $Co(dmgBF_2)_2L_2$-mediated HOR were undertaken with the goal of determining whether this approximate rate law is appropriate and, if so, to measure the rate constants related to each pathway. By better understanding the bifurcation between these two pathways, insight may be gained into the microscopic-reverse HER.

$$(6) \qquad \frac{d[Co^I]^-}{dt} = \left\{K_1 k_2 + K_1 K_3 k_4 \frac{[B]}{[HB^+]}\right\}[Co^{II}]^2[H_2]$$

Selection of Base and Initial Kinetic Experiments

Co(II) species are kinetically labile, and cobaloximes in this oxidation state rapidly exchange axial ligands. In order to simplify kinetic analysis and avoid solution speciation, a non-coordinating base was sought which would ensure that solvent was the only source of spectator axial ligands. The optical spectra of $Co(dmgBF_2)_2(MeCN)_2$ solutions in MeCN were not altered by addition of *N,N*-dimethylaniline or 1,8-bis(dimethylamino)naphthalene ("proton sponge"), indicating neither displaces axial MeCN. Proton sponge is a relatively strong base (conjugate acid pK_a in MeCN = 18.2[41]), which favors the products side of the equilibrium, and an easy-to-handle solid at room temperature, making it an ideal candidate for initial studies.

Addition of an atmosphere of H_2 to a MeCN solution containing $Co(dmgBF_2)_2(MeCN)_2$ and excess proton sponge resulted in the appearance of optical bands at 553 and 628 nm, consistent with the known spectrum of $[Co(dmgBF_2)_2MeCN]^-$ after an induction period of three hours (Figure 2).[26] The $[Co(dmgBF_2)_2MeCN]^-$ spectrum continued to grow in isosbestically over the course of three days until all of the $Co(dmgBF_2)_2(MeCN)_2$ had been converted to $[Co(dmgBF_2)_2MeCN]^-$. The reaction did not reverse when the H_2 atmosphere was removed and was not altered by the presence of the conjugate acid.

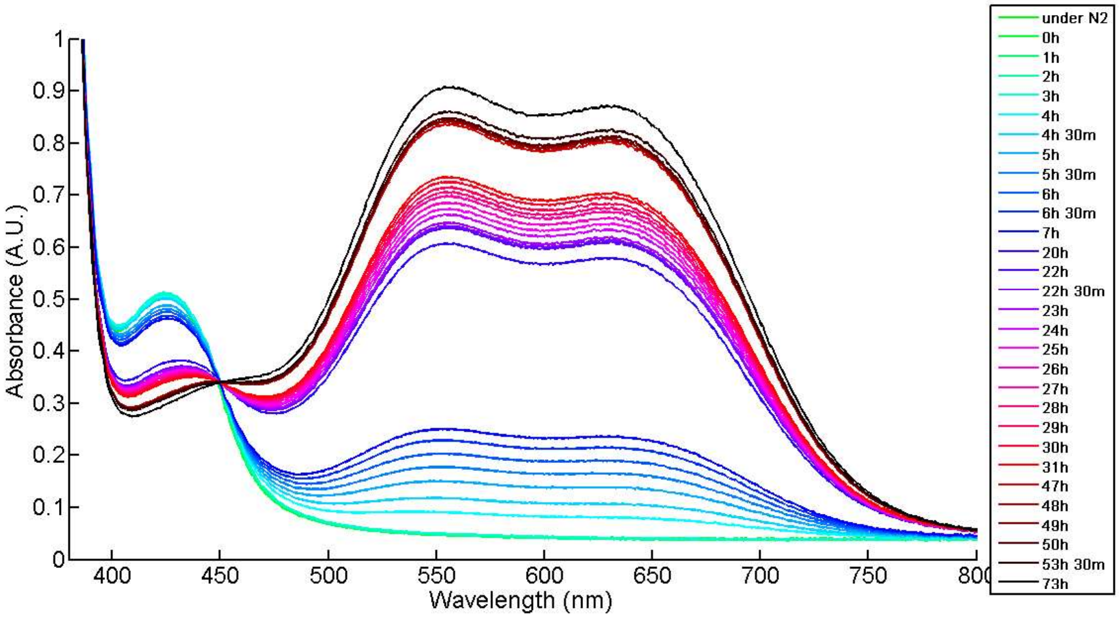

Figure 2: Time-dependent optical spectra of 1.9 mM $\mathrm{Co(dmgBF_2)_2(MeCN)_2}$ and 36 mM proton sponge in MeCN under 1 atm H_2.

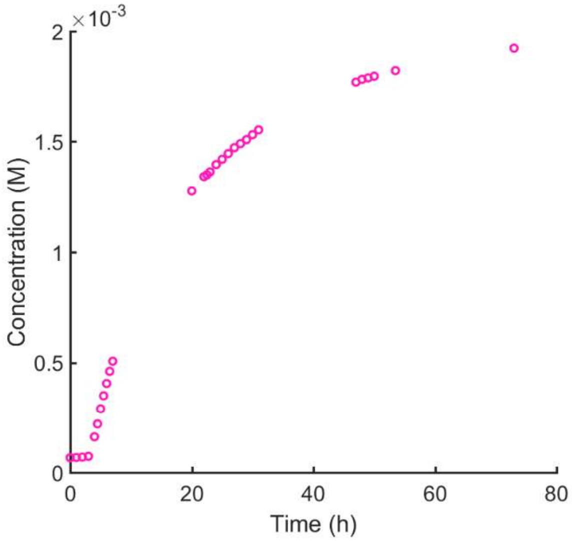

Figure 3: Concentration of Co(I) over time based on absorption at 553 nm.

Varying the concentration of both the Co species and the base produced variable induction periods with no distinct pattern, but all reactions proceeded to completion over the course of 2-3 days. Plots of the natural logarithm, inverse, and inverse-square of concentration vs. time were all nonlinear even when the induction period was excluded from the data.

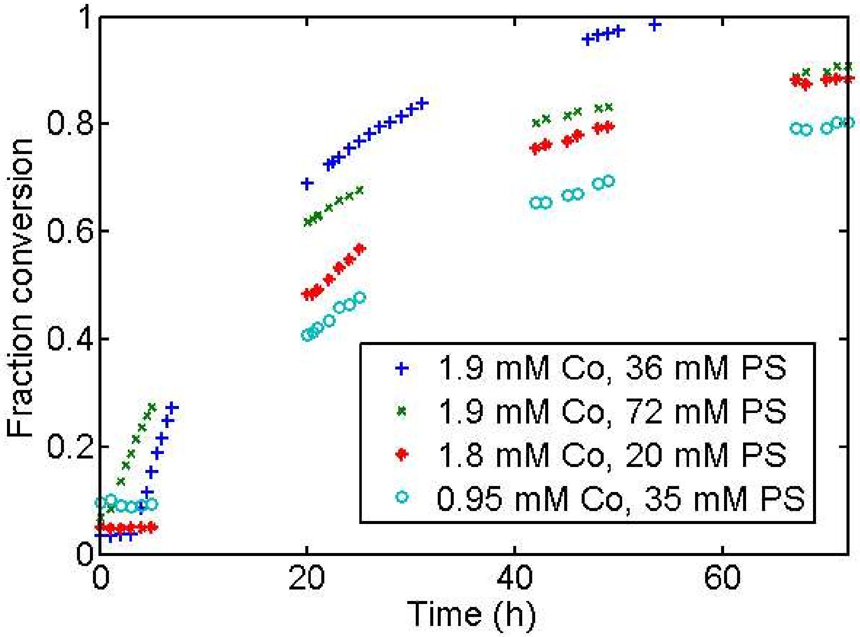

Figure 4: Comparison of data from runs with different initial concentrations of Co(dmgBF$_2$)$_2$(MeCN)$_2$ (Co) and proton sponger (PS).

Initial Rate Experiments Using Proton Sponge

The initial rate method is ideal for studying slow reactions, and was pursued along with higher concentration experiments to expedite data collection (Table 1, additional data in Supporting Data). The initial concentration of each reactant was systematically varied, and the average of a linear fit of the absorption data for the two Co(I) bands used to calculate the initial rate for each condition, truncating any observed induction period. The initial rate was not affected by variations in initial concentration of proton sponge. However, doubling the initial pressure of H_2 resulted in a doubling of the initial rate, and the initial rate varied with variations in the initial concentration of $Co(dmgBF_2)_2(MeCN)_2$. A natural log-log plot of the initial rate vs. concentration was linear with a slope of 2.03 (Figure 5).

Table 1: Initial rate data for the reaction of $Co(dmgBF_2)_2(MeCN)_2$ (Co), proton sponge (B) and H_2.

Entry	$[Co]_0$ (mM)	$[B]_0$ (mM)	$P(H_2)$ (atm)	Initial Rate (M/s x 10^7)
1	5.8	8.5	1.0	3.4
2	6.0	4.3	1.0	3.3
3	6.0	2.1	1.0	3.2
4	4.6	2.2	1.0	1.9
5	3.0	2.1	1.0	0.91
6	1.7	2.2	1.0	0.23
7	5.8	25.2	1.0	4.4
8	6.2	19.7	0.50	1.9
9	6.3	19.7	0.25	0.86

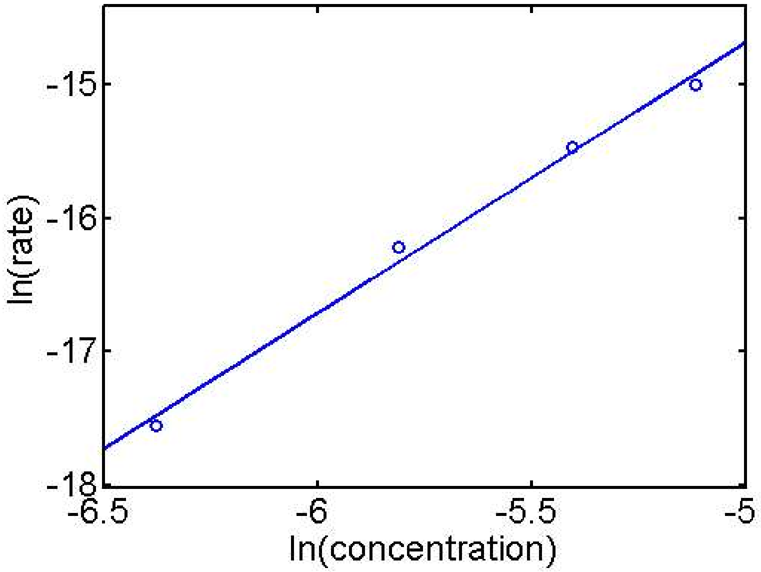

Figure 5: Rate vs. concentration log-log plot for Co-varied runs and fit line. Slope = 2.03, $R^2 = 0.999$.

Extension to N,N-dimethylaniline

Further initial rate experiments were pursued using *N,N*-dimethylaniline in order to understand the effect of base strength (conjugate acid pK_a in MeCN = 11.4[42]) on the kinetics of $Co(dmgBF_2)_2(MeCN)_2$-mediated HOR. Induction periods prior to the appearance of $[Co(dmgBF_2)_2MeCN]^-$ bands were frequently observed. The concentration vs. time data became nonlinear within minutes, and the reaction did not proceed to completion after 24 h. After three days, the solution had reached equilibrium with an equilibrium constant of 1.3 x 10^{-5} $atm^{-1/2}$. Removal of H_2 resulted in a slow diminution of the $[Co(dmgBF_2)_2MeCN]^-$ spectrum.

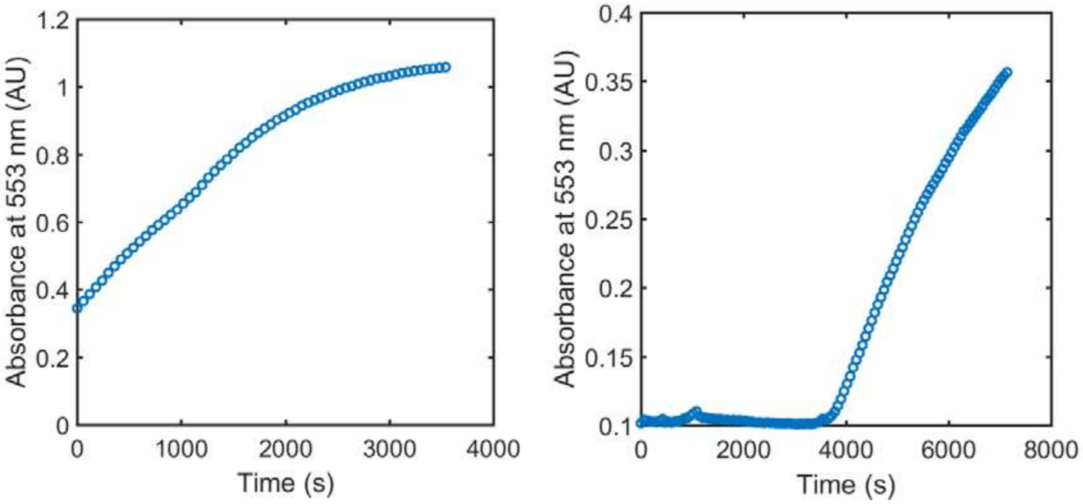

Figure 6: Example plots of absorbance over time for Co(dmgBF-$_2$)$_2$(MeCN)$_2$ and *N,N*-dimethylaniline under H_2.

Discussion

Observed Induction Period

The variable induction periods observed in these experiments likely occur due to trace O_2 present in solution. Blue solutions of [Co(dmgBF$_2$)$_2$MeCN]$^-$ are rapidly converted to yellow Co(dmgBF$_2$)$_2$(MeCN)$_2$ on exposure to air, and the induction periods observed were considerably longer when an ordinary Schlenk line (pressure ca. 50 mTorr) was used to degas the reaction vessel than when a high vacuum line (pressure ca. 5 μTorr) was used. The induction period is then produced by rapid reoxidation of [Co(dmgBF$_2$)$_2$MeCN]$^-$ as it is produced at early time points. If this is the case, initial rate data recorded after the induction period ends should still be valid, since the reaction of interest is rate-limiting and therefore the induction period is simply obscuring the beginning of the linear data region. However, rigorous exclusion of oxygen or monitoring of the production of products not affected by trace oxygen (i.e. conjugate acid) would be desirable to verify this hypothesis and ensure the reliablility of the data collected. Additionally, for experiments with bases such as *N,N*-dimethylaniline which approach equilibrium rapidly relative to the length of the induction period, enough of the linear data region may be obscured to render initial rates difficult to reliably extract.

The source of the O_2 is unclear, as solutions were prepared in a nitrogen-filled glovebox in Kontes valve-equipped cuvettes which were sufficiently gastight to prevent detectable leakage of H_2 and degassed on a high-vacuum line before H_2 addition from a line flushed with gas for several minutes. These conditions would ordinarily be considered rigorously free of O_2; it is possible that this reaction is simply slow enough to observe the effects of unavoidable traces of O_2 which remain despite the most rigorous efforts to eliminate it.

Rate Law of HOR

The initial rate data for $Co(dmgBF_2)_2(MeCN)_2$-mediated HOR indicates a reaction that is second-order in Co, first-order in H_2, and zero-order in proton sponge, with a rate constant of 3.8 ± .5 $M^{-2}s^{-1}$. This rate law suggests that only the homolytic pathway is accessed in this reaction, and the rate constant is smaller by two orders of magnitude than that measured by Norton with radical scavengers.[40]

The complete dominance of the homolytic pathway is unexpected, given that proton sponge is sufficiently basic to make the reaction irreversible, as evidenced by the final concentration of $[Co(dmgBF_2)_2MeCN]^-$ being equal to the initial concentration of $Co(dmgBF_2)_2(MeCN)_2$, the observation that the reaction does not reverse when the H_2 atmosphere is removed, and the lack of any effect on the reaction when the conjugate acid is present in solution. It is possible, then, that the pK_a of the Co(III) hydride species is less than 18.2 in MeCN, but the pK_a of the dihydrogen adduct is much higher. Recent work examining the relationship between acid identity and hydride formation rates in a related Co complex identified a departure from the linear free energy relationship with pK_a when the acidic proton is sterically encumbered, as in *N,N*-dimethylanilinium.[43] It is therefore also possible that the selection of a sterically encumbered base in order to preclude solution speciation has resulted in a much slower deprotonation rate than would be expected based on pH, to the point where heterolysis cannot compete with homolysis.

Further research would be needed to distinguish these effects. Alternate strategies for circumventing solution speciation, such as using a strong non-solvent axial ligand to push the speciation equilibrium far to one side or operating in a noncoordinating solvent such as CH_2Cl_2 would allow for unencumbered bases to be examined and analyzed unambiguously based on conjugate acid pK_a.

Conclusion

Initial rate data suggests that the HOR mediated by $Co(dmgBF_2)_2(MeCN)_2$ using proton sponge as the base proceeds by homolytic cleavage of the H-H bond. More experiments varying the base are needed to contextualize these results, as well as better methodology with respect to the exclusion of oxygen.

References

(1) Schrauzer, G. N.; Windgassen, R. J. Über Cobaloxime(II) Und Deren Beziehung Zum Vitamin B12r. *Chem. Ber.* **1966**, *99* (2), 602–610. https://doi.org/10.1002/cber.19660990234.

(2) Schrauzer, G. N.; Windgassen, R. J. Alkylcobaloximes and Their Relation to Alkylcobalamins. *J. Am. Chem. Soc.* **1966**, *88* (16), 3738–3743. https://doi.org/10.1021/ja00968a012.

(3) Razavet, M.; Artero, V.; Fontecave, M. Proton Electroreduction Catalyzed by Cobaloximes: Functional Models for Hydrogenases. *Inorg. Chem.* **2005**, *44* (13), 4786–4795. https://doi.org/10.1021/ic050167z.

(4) Connolly, P.; Espenson, J. H. Cobalt-Catalyzed Evolution of Molecular Hydrogen. *Inorg. Chem.* **1986**, *25* (16), 2684–2688. https://doi.org/10.1021/ic00236a006.

(5) Dempsey, J. L.; Brunschwig, B. S.; Winkler, J. R.; Gray, H. B. Hydrogen Evolution Catalyzed by Cobaloximes. *Acc. Chem. Res.* **2009**, *42* (12), 1995–2004. https://doi.org/10.1021/ar900253e.

(6) Hu, X.; Cossairt, B. M.; Brunschwig, B. S.; Lewis, N. S.; Peters, J. C. Electrocatalytic Hydrogen Evolution by Cobalt Difluoroboryl-Diglyoximate Complexes. *Chem. Commun.* **2005**, No. 37, 4723–4725. https://doi.org/10.1039/B509188H.

(7) Zhang, P.; Jacques, P.-A.; Chavarot-Kerlidou, M.; Wang, M.; Sun, L.; Fontecave, M.; Artero, V. Phosphine Coordination to a Cobalt Diimine–Dioxime Catalyst Increases Stability during Light-Driven H2 Production. *Inorg. Chem.* **2012**, *51* (4), 2115–2120. https://doi.org/10.1021/ic2019132.

(8) Li, L.; Duan, L.; Wen, F.; Li, C.; Wang, M.; Hagfeldt, A.; Sun, L. Visible Light Driven Hydrogen Production from a Photo-Active Cathode Based on a Molecular Catalyst and Organic Dye-Sensitized p-Type Nanostructured NiO. *Chem. Commun.* **2012**, *48* (7), 988–990. https://doi.org/10.1039/C2CC16101J.

(9) Guttentag, M.; Rodenberg, A.; Kopelent, R.; Probst, B.; Buchwalder, C.; Brandstätter, M.; Hamm, P.; Alberto, R. Photocatalytic H2 Production with a Rhenium/Cobalt System in Water under Acidic Conditions. *Eur. J. Inorg. Chem.* **2012**, *2012* (1), 59–64. https://doi.org/10.1002/ejic.201100883.

(10) Utschig, L. M.; Silver, S. C.; Mulfort, K. L.; Tiede, D. M. Nature-Driven Photochemistry for Catalytic Solar Hydrogen Production: A Photosystem I–Transition Metal Catalyst Hybrid. *J. Am. Chem. Soc.* **2011**, *133* (41), 16334–16337. https://doi.org/10.1021/ja206012r.

(11) Probst, B.; Guttentag, M.; Rodenberg, A.; Hamm, P.; Alberto, R. Photocatalytic H2 Production from Water with Rhenium and Cobalt Complexes. *Inorg. Chem.* **2011**, *50* (8), 3404–3412. https://doi.org/10.1021/ic102317u.

(12) McCormick, T. M.; Han, Z.; Weinberg, D. J.; Brennessel, W. W.; Holland, P. L.; Eisenberg, R. Impact of Ligand Exchange in Hydrogen Production from Cobaloxime-Containing Photocatalytic Systems. *Inorg. Chem.* **2011**, *50* (21), 10660–10666. https://doi.org/10.1021/ic2010166.

(13) Dong, J.; Wang, M.; Zhang, P.; Yang, S.; Liu, J.; Li, X.; Sun, L. Promoting Effect of Electrostatic Interaction between a Cobalt Catalyst and a Xanthene Dye on Visible-Light-Driven Electron Transfer and Hydrogen Production. *J. Phys. Chem. C* **2011**, *115* (30), 15089–15096. https://doi.org/10.1021/jp2040778.

(14) Zhang, P.; Wang, M.; Dong, J.; Li, X.; Wang, F.; Wu, L.; Sun, L. Photocatalytic Hydrogen Production from Water by Noble-Metal-Free Molecular Catalyst Systems Containing Rose Bengal and the Cobaloximes of BFx-Bridged Oxime Ligands. *J. Phys. Chem. C* **2010**, *114* (37), 15868–15874. https://doi.org/10.1021/jp106512a.

(15) Zhang, P.; Wang, M.; Li, C.; Li, X.; Dong, J.; Sun, L. Photochemical H2 Production with Noble-Metal-Free Molecular Devices Comprising a Porphyrin Photosensitizer and a Cobaloxime Catalyst. *Chem. Commun.* **2009**, *46* (46), 8806–8808. https://doi.org/10.1039/C0CC03154B.

(16) Probst, B.; Rodenberg, A.; Guttentag, M.; Hamm, P.; Alberto, R. A Highly Stable Rhenium−Cobalt System for Photocatalytic H2 Production: Unraveling the Performance-Limiting Steps. *Inorg. Chem.* **2010**, *49* (14), 6453–6460. https://doi.org/10.1021/ic100036v.

(17) Berben, L. A.; Peters, J. C. Hydrogen Evolution by Cobalt Tetraimine Catalysts Adsorbed on Electrode Surfaces. *Chem. Commun.* **2010**, *46* (3), 398–400. https://doi.org/10.1039/B921559J.

(18) Probst, B.; Kolano, C.; Hamm, P.; Alberto, R. An Efficient Homogeneous Intermolecular Rhenium-Based Photocatalytic System for the Production of H2. *Inorg. Chem.* **2009**, *48* (5), 1836–1843. https://doi.org/10.1021/ic8013255.

(19) Du, P.; Schneider, J.; Luo, G.; Brennessel, W. W.; Eisenberg, R. Visible Light-Driven Hydrogen Production from Aqueous Protons Catalyzed by Molecular Cobaloxime Catalysts. *Inorg. Chem.* **2009**, *48* (11), 4952–4962. https://doi.org/10.1021/ic900389z.

(20) Hu, X.; Brunschwig, B. S.; Peters, J. C. Electrocatalytic Hydrogen Evolution at Low Overpotentials by Cobalt Macrocyclic Glyoxime and Tetraimine Complexes. *J. Am. Chem. Soc.* **2007**, *129* (29), 8988–8998. https://doi.org/10.1021/ja067876b.

(21) Schrauzer, G. N.; Holland, R. J. Hydridocobaloximes. *J. Am. Chem. Soc.* **1971**, *93* (6), 1505–1506. https://doi.org/10.1021/ja00735a040.

(22) Bhattacharjee, A.; Chavarot-Kerlidou, M.; Andreiadis, Eugen. S.; Fontecave, M.; Field, M. J.; Artero, V. Combined Experimental–Theoretical Characterization of the Hydrido-Cobaloxime [HCo(DmgH)2(PnBu3)]. *Inorg. Chem.* **2012**, *51* (13), 7087–7093. https://doi.org/10.1021/ic2024204.

(23) Lacy, D. C.; Roberts, G. M.; Peters, J. C. The Cobalt Hydride That Never Was: Revisiting Schrauzer's "Hydridocobaloxime." *J. Am. Chem. Soc.* **2015**, *137* (14), 4860–4864. https://doi.org/10.1021/jacs.5b01838.

(24) Chao, T.-H.; Espenson, J. H. Mechanism of Hydrogen Evolution from Hydridocobaloxime. *J. Am. Chem. Soc.* **1978**, *100* (1), 129–133. https://doi.org/10.1021/ja00469a022.

(25) Szajna-Fuller, E.; Bakac, A. Catalytic Generation of Hydrogen with Titanium Citrate and a Macrocyclic Cobalt Complex. *Eur. J. Inorg. Chem.* **2010**, *2010* (17), 2488–2494. https://doi.org/10.1002/ejic.200901176.

(26) Dempsey, J. L.; Winkler, J. R.; Gray, H. B. Mechanism of H2 Evolution from a Photogenerated Hydridocobaloxime. *J. Am. Chem. Soc.* **2010**, *132* (47), 16774–16776. https://doi.org/10.1021/ja109351h.

(27) Wiedner, E. S.; Bullock, R. M. Electrochemical Detection of Transient Cobalt Hydride Intermediates of Electrocatalytic Hydrogen Production. *J. Am. Chem. Soc.* **2016**, *138* (26), 8309–8318. https://doi.org/10.1021/jacs.6b04779.

(28) Rountree, E. S.; Martin, D. J.; McCarthy, B. D.; Dempsey, J. L. Linear Free Energy Relationships in the Hydrogen Evolution Reaction: Kinetic Analysis of a Cobaloxime Catalyst. *ACS Catal.* **2016**, *6* (5), 3326–3335. https://doi.org/10.1021/acscatal.6b00667.

(29) McCrory, C. C. L.; Uyeda, C.; Peters, J. C. Electrocatalytic Hydrogen Evolution in Acidic Water with Molecular Cobalt Tetraazamacrocycles. *J. Am. Chem. Soc.* **2012**, *134* (6), 3164–3170. https://doi.org/10.1021/ja210661k.

(30) Estes, D. P.; Grills, D. C.; Norton, J. R. The Reaction of Cobaloximes with Hydrogen: Products and Thermodynamics. *J. Am. Chem. Soc.* **2014**, *136* (50), 17362–17365. https://doi.org/10.1021/ja508200g.

(31) Simándi, L. I.; Budó-Záhonyi, É.; Szeverényi, Z. Effect of Strong Base on the Activation of Molecular Hydrogen by Pyridinebis(Dimethylglyoximato)Cobalt(II). *Inorg. Nucl. Chem. Lett.* **1976**, *12* (3), 237–241. https://doi.org/10.1016/0020-1650(76)80158-4.

(32) Simándi, L. I.; Szeverényi, Z.; Budó-Záhonyi, É. Activation of Molecular Hydrogen by Cobaloxime(II) Derivatives. *Inorg. Nucl. Chem. Lett.* **1975**, *11* (11), 773–777. https://doi.org/10.1016/0020-1650(75)80098-5.

(33) Yamaguchi, T.; Miyagawa, R. The Effect of Pyridine on the Hydrogen Absorption Process of Bis(Dimethylglyoximato)Cobalt(Ii). *Chem. Lett.* **1978**, *7* (1), 89–92. https://doi.org/10.1246/cl.1978.89.

(34) Yamaguchi, T.; Tsumura, T. The Effect of Triphenylphosphine on the Hydrogenation Reaction of Bis(Dimethylglyoximato)Cobalt(Ii). *Chem. Lett.* **1973**, *2* (4), 409–412. https://doi.org/10.1246/cl.1973.409.

(35) Yamaguchi, T.; Nakayama, M.; Tsumura, T. The Effect of Base Strength of Schiff Bases on Their Catalytic Hydrogenation with Bis(Dimethylglyoximato)Cobalt(Ii). *Chem. Lett.* **1972**, *1* (12), 1231–1234. https://doi.org/10.1246/cl.1972.1231.

(36) Lawrence, M. A. W.; Celestine, M. J.; Artis, E. T.; Joseph, L. S.; Esquivel, D. L.; Ledbetter, A. J.; Cropek, D. M.; Jarrett, W. L.; Bayse, C. A.; Brewer, M. I.; et al. Computational, Electrochemical, and Spectroscopic Studies of Two Mononuclear Cobaloximes: The Influence of an Axial Pyridine and Solvent on the Redox Behaviour and Evidence for Pyridine Coordination to Cobalt(I) and Cobalt(II) Metal Centres. *Dalton Trans.* **2016**, *45* (25), 10326–10342. https://doi.org/10.1039/C6DT01583B.

(37) Basu, D.; Mazumder, S.; Niklas, J.; Baydoun, H.; Wanniarachchi, D.; Shi, X.; Staples, R. J.; Poluektov, O.; Schlegel, H. B.; Verani, C. N. Evaluation of the Coordination Preferences and Catalytic Pathways of Heteroaxial Cobalt Oximes towards Hydrogen Generation. *Chem. Sci.* **2016**, *7* (5), 3264–3278. https://doi.org/10.1039/C5SC04214C.

(38) Panagiotopoulos, A.; Ladomenou, K.; Sun, D.; Artero, V.; Coutsolelos, A. G. Photochemical Hydrogen Production and Cobaloximes: The Influence of the Cobalt Axial N-Ligand on the System Stability. *Dalton Trans.* **2016**, *45* (15), 6732–6738. https://doi.org/10.1039/C5DT04502A.

(39) Li, G.; Estes, D. P.; Norton, J. R.; Ruccolo, S.; Sattler, A.; Sattler, W. Dihydrogen Activation by Cobaloximes with Various Axial Ligands. *Inorg. Chem.* **2014**, *53* (19), 10743–10747. https://doi.org/10.1021/ic501975r.

(40) Li, G.; Han, A.; Pulling, M. E.; Estes, D. P.; Norton, J. R. Evidence for Formation of a Co–H Bond from (H2O)2Co(DmgBF2)2 under H2: Application to Radical Cyclizations. *J. Am. Chem. Soc.* **2012**, *134* (36), 14662–14665. https://doi.org/10.1021/ja306037w.

(41) Ozeryanskii, V. A.; Pozharskii, A. F.; Milgizina, G. R.; Howard, S. T. Synthesis and Properties of 5,6-Bis(Dimethylamino)Acenaphthylene: The First Proton Sponge with Easily-Modified Basicity. *J. Org. Chem.* **2000**, *65* (22), 7707–7709. https://doi.org/10.1021/jo001171p.

(42) Tshepelevitsh, S.; Kütt, A.; Lõkov, M.; Kaljurand, I.; Saame, J.; Heering, A.; Plieger, P. G.; Vianello, R.; Leito, I. On the Basicity of Organic Bases in Different Media. *Eur. J. Org. Chem.* **2019**, *2019* (40), 6735–6748. https://doi.org/10.1002/ejoc.201900956.

(43) Elgrishi, N.; Kurtz, D. A.; Dempsey, J. L. Reaction Parameters Influencing Cobalt Hydride Formation Kinetics: Implications for Benchmarking H2-Evolution Catalysts. *J. Am. Chem. Soc.* **2017**, *139* (1), 239–244. https://doi.org/10.1021/jacs.6b10148.

(44) Pangborn, A. B.; Giardello, M. A.; Grubbs, R. H.; Rosen, R. K.; Timmers, F. J. Safe and Convenient Procedure for Solvent Purification. *Organometallics* **1996**, *15* (5), 1518–1520. https://doi.org/10.1021/om9503712.

Methods

General Considerations

Unless stated otherwise, all manipulations were carried out in a nitrogen-filled glovebox or under nitrogen or argon using standard Schlenk techniques. Dry, air-free solvents were obtained from a Grubbs-type solvent purification system.[44] $Co(dmgBF_2)_2(MeCN)_2$ was synthesized by a literature method[26] and its purity confirmed by cyclic voltammetry prior to use. Proton sponge and *N,N*-dimethylaniline were ordered from Sigma-Aldrich and used as received. UV-Vis spectra were recorded on a Cary Bio 50 spectrometer.

General Procedure for Kinetics Experiments

A solution of $Co(dmgBF_2)_2(MeCN)_2$ and base (proton sponge or *N,N*-dimethylaniline) was prepared in MeCN. A 1 mm path length, Kontes valve-sealed cuvette equipped with a side-arm bulb and a stirbar was charged with the solution and degassed on a high-vacuum line by the freeze-pump-thaw method twice. The solution was allowed to warm to room temperature before H_2 was added to the desired pressure. The reaction was monitored by UV-Vis spectroscopy by tipping the solution into the cuvette at the desired intervals and was stirred in the side-arm bulb between spectra.

Supporting Data

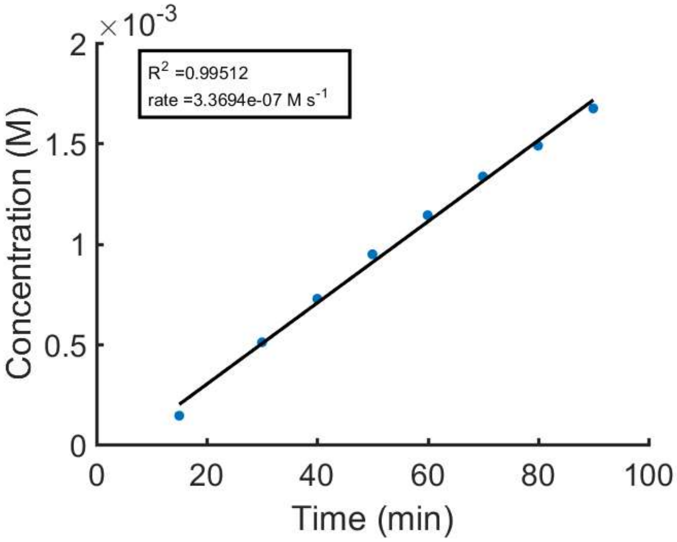

Figure S1: Initial rate plot for Table 1 entry 1, calculated based on absorbance at 553 nm.

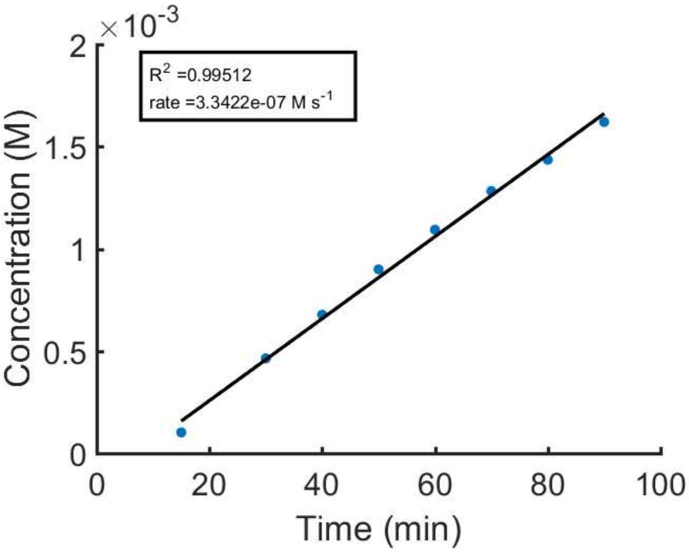

Figure S2: Initial rate plot for Table 1 entry 1, calculated based on absorbance at 628 nm.

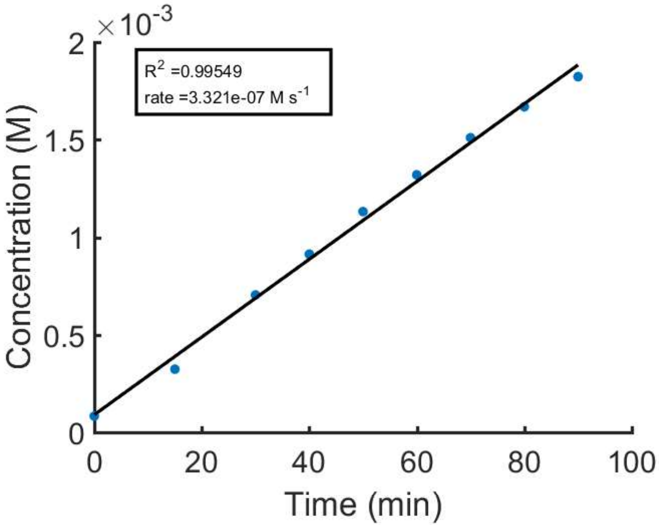

Figure S3: Initial rate plot for Table 1 entry 2, calculated based on absorbance at 553 nm.

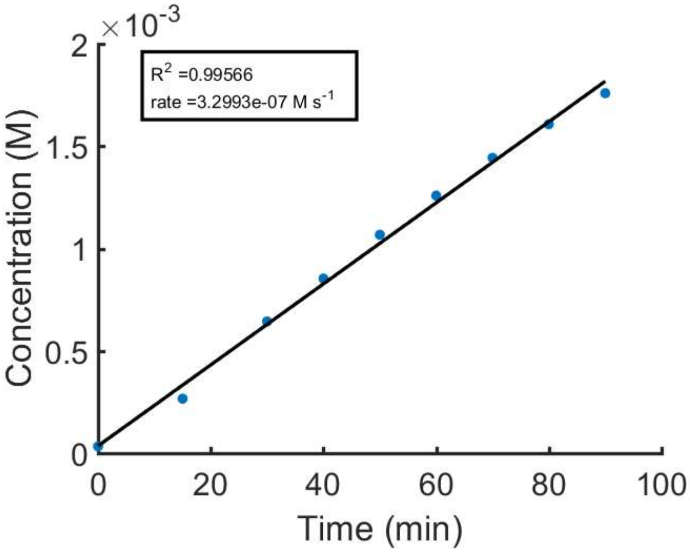

Figure S4: Initial rate plot for Table 1 entry 2, calculated based on absorbance at 628 nm.

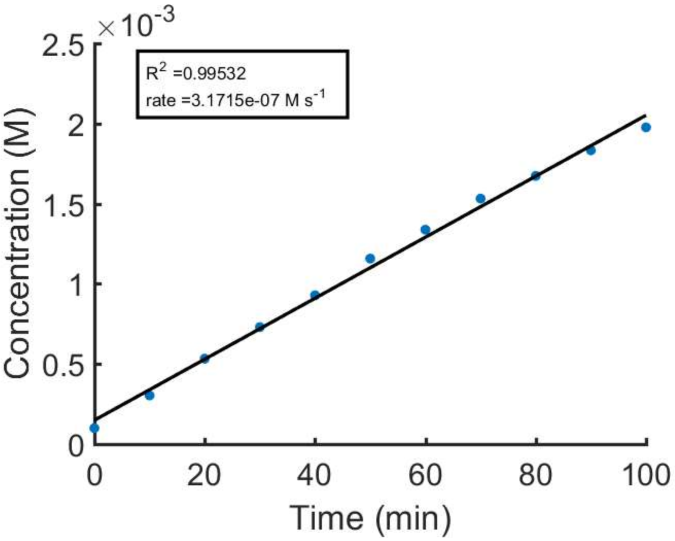

Figure S5: Initial rate plot for Table 1 entry 3, calculated based on absorbance at 553 nm.

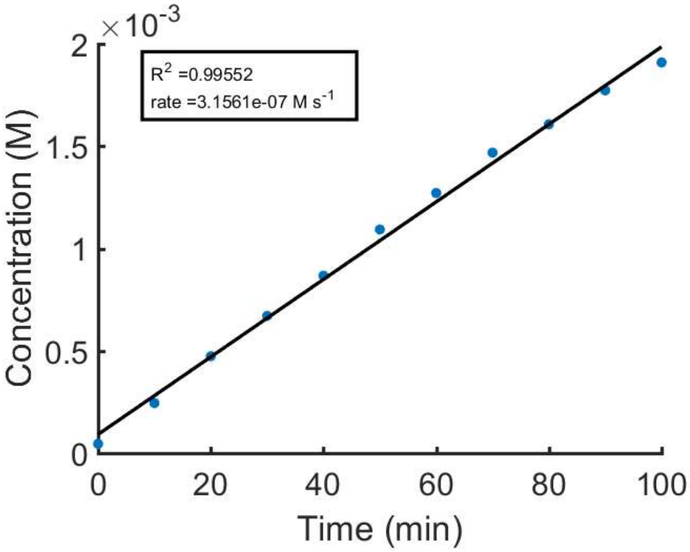

Figure S6: Initial rate plot for Table 1 entry 3, calculated based on absorbance at 628 nm.

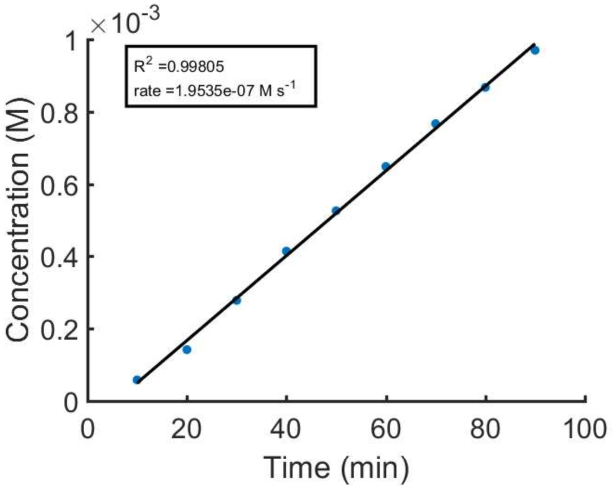

Figure S7: Initial rate plot for Table 1 entry 4, calculated based on absorbance at 553 nm.

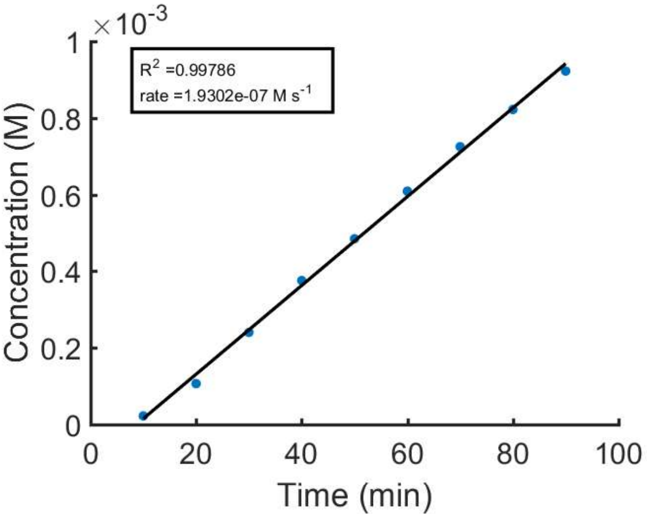

Figure S8: Initial rate plot for Table 1 entry 4, calculated based on absorbance at 628 nm.

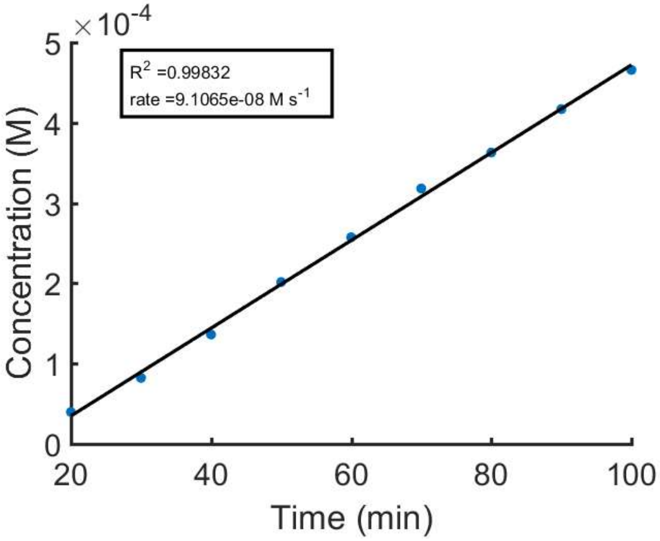

Figure S9: Initial rate plot for Table 1 entry 5, calculated based on absorbance at 553 nm.

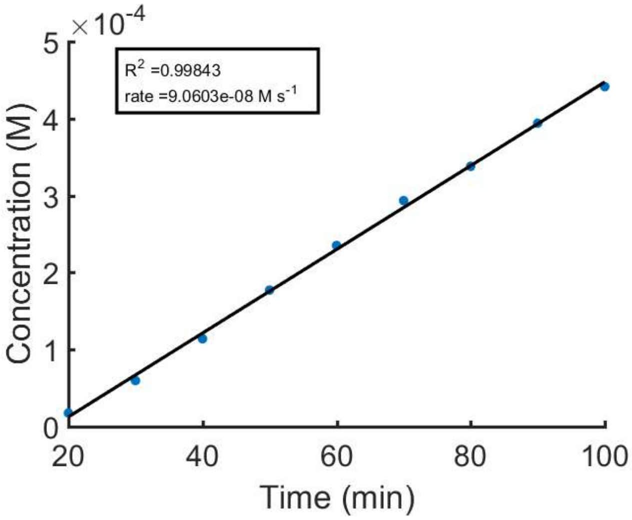

Figure S10: Initial rate plot for Table 1 entry 5, calculated based on absorbance at 628 nm.

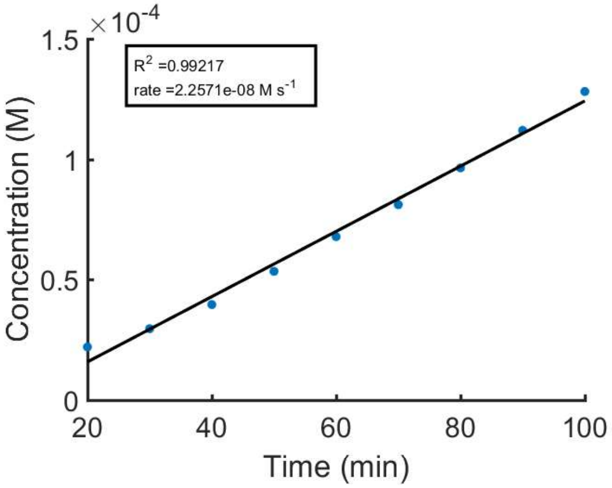

Figure S11: Initial rate plot for Table 1 entry 6, calculated based on absorbance at 553 nm.

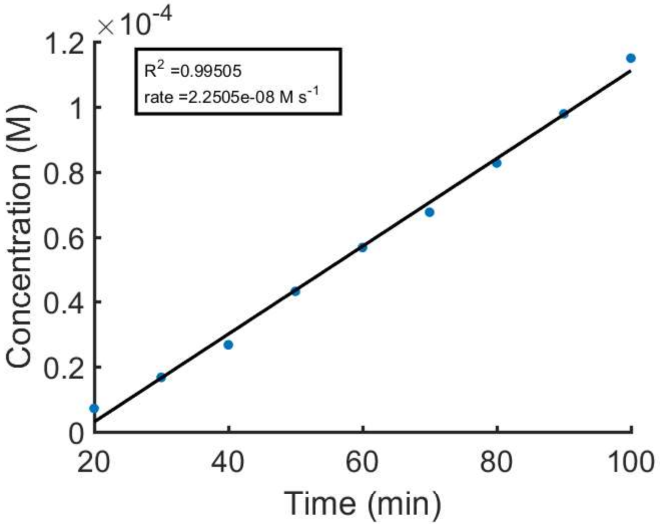

Figure S12: Initial rate plot for Table 1 entry 6, calculated based on absorbance at 628 nm.

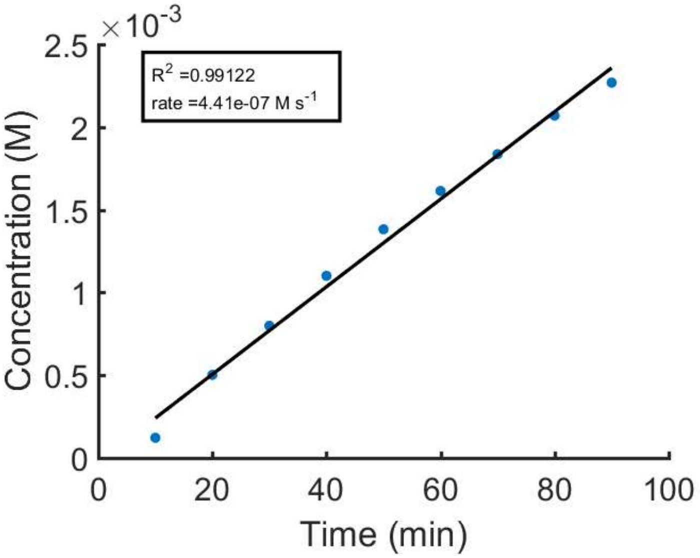

Figure S13: Initial rate plot for Table 1 entry 7, calculated based on absorbance at 553 nm.

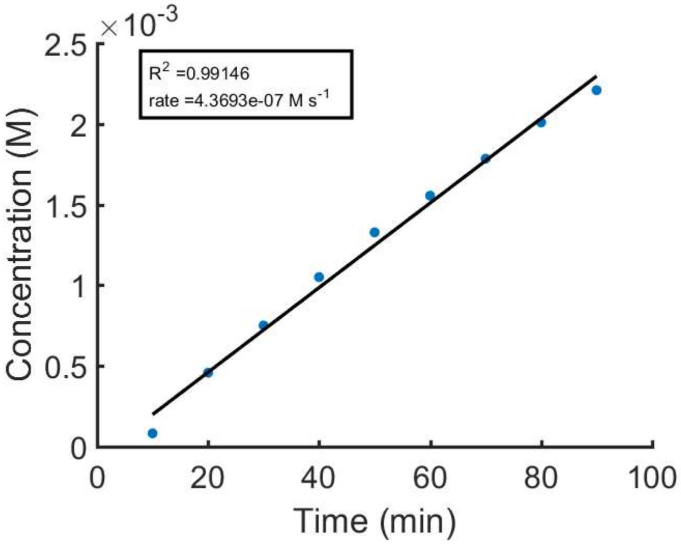

Figure S14: Initial rate plot for Table 1 entry 7, calculated based on absorbance at 628 nm.

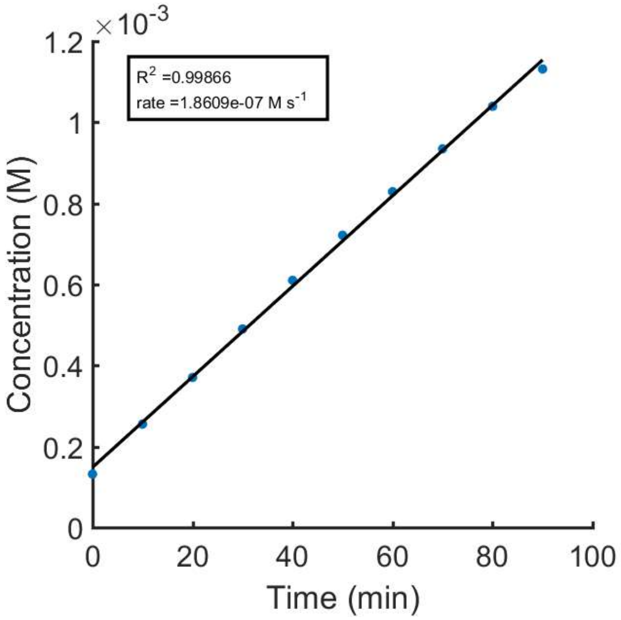

Figure S15: Initial rate plot for Table 1 entry 8, calculated based on absorbance at 553 nm.

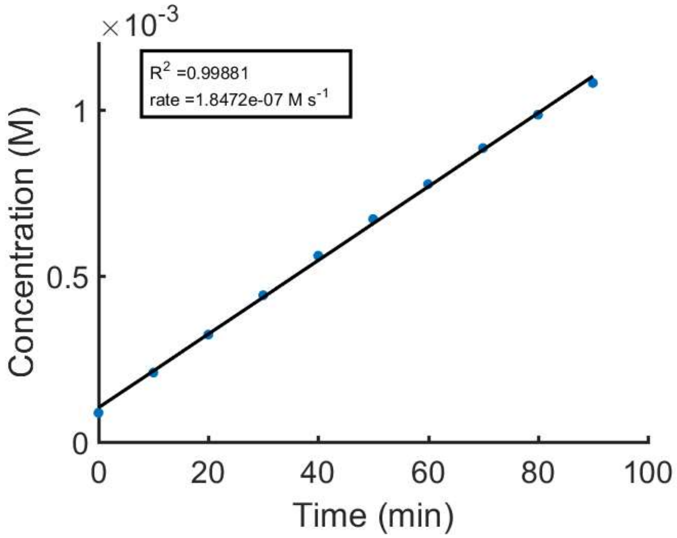

Figure S16: Initial rate plot for Table 1 entry 8, calculated based on absorbance at 628 nm.

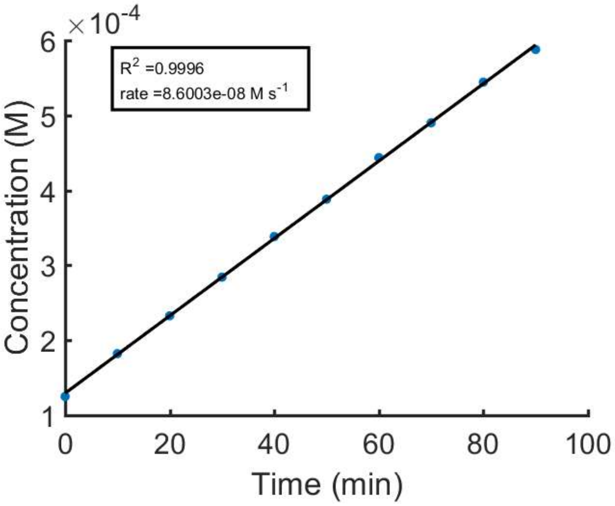

Figure S17: Initial rate plot for Table 1 entry 9, calculated based on absorbance at 553 nm

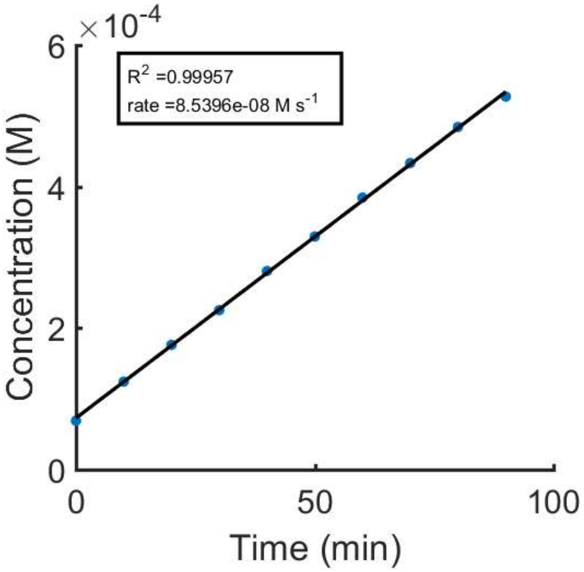

Figure S18: Initial rate plot for Table 1 entry 9, calculated based on absorbance at 628 nm.